Non-Covalent Self-Assembly and Covalent Polymerization Co-Contribute to Polydopamine Formation

Seonki Hong, Yun Suk Na, Sunghwan Choi, In Taek Song, Woo Youn Kim, and Haeshin Lee**

Polydopamine is the first adhesive polymer that can functionalize surfaces made of virtually all material chemistries. The material-independent surface modification properties of polydopamine allow the functionalization of various types of medical and energy devices. However, the mechanism of dopamine polymerization has not yet been clearly demonstrated. Covalent oxidative polymerization via 5,6-dihydroxyindole (DHI), which is similar to the mechanism for synthetic melanin synthesis, has been the clue. Here, it is reported that a physical, self-assembled trimer of (dopamine)$_2$/DHI exists in polydopamine, which has been known to be formed only by covalent polymerization. It is also found that the trimeric complex is tightly entrapped within polydopamine and barely escapes from the polydopamine complex. The result explains the previously reported in vitro and in vivo biocompatibility. The study reveals a different perspective of polydopamine formation, where it forms in part by the self-assembly of dopamine and DHI, providing a new clue toward understanding the structures of catecholamines such as melanin.

1. Introduction

Polydopamine coating is a rapidly emerging method to precisely control surface properties. The invention of polydopamine coating was inspired by the adhesive properties of marine mussels.[1] Since it was first reported in Oct. 2007, polydopamine coatings have been widely exploited in a variety of fields, including biomineralization,[2–4] single-cell encapsulation,[5] soft-lithography,[6,7] biocompatible surface modifications,[8–10] attenuation of intrinsic in vivo toxicity of biomaterials,[11] nanomaterial functionalization,[14–17] Li-ion batteries,[18] neural interfaces,[19] sensors,[20] catalysts,[21–23] and others.[24,25] The wide ranges of applications result from the unique properties of polydopamine. Polydopamine allows it to be applied to virtually any type of surface, regardless of the material's chemistry, and takes advantage of its intrinsic chemical reactivity with nucleophiles, its ability to chelate metal ions, and its redox activities.[26] Polydopamine is spontaneously formed by pH-induced, oxidative polymerization of dopamine-hydrochloride in alkaline solutions (pH > 7.5).

Despite the widespread use of polydopamine, the molecular mechanism behind polydopamine formation has not been fully investigated. It has been suggested that polydopamine formation shares many characteristics with melanin biosynthesis pathways.[27] Melanin biosynthesis includes an oxidative reaction pathway, which transforms dopamine into 5,6-dihydroxyindole (DHI), followed by further polymerization steps. The exact structure of melanin is also unclear, but the intermediates have been studied in relation to DHI chemistry, forming covalently bonded DHI dimers, trimers, tetramers, and their subsequent heterogeneous aggregates.[28–33] The previously reported structure of polydopamine was suggested to follow the DHI chemistry that was similar to melanin biosynthesis. This led to the assumption that the brown-black color of polydopamine is formed by a covalently bonded polymer.[1]

Here we report that the physical self-assembly of dopamine and its oxidative product, 5,6-dihydroxyindole (DHI), contribute to polydopamine formation. We found that a significant amount of dopamine remains unpolymerized as a self-assembled stable complex of (dopamine)$_2$/DHI (**Scheme 1**B). The previously proposed oxidative polymerization occurred in parallel with this self-assembly (Scheme 1A), providing the first evidence that polydopamine is formed through two different pathways, non-covalent self-assembly and covalent polymerization. A large amount of the dopamine/DHI complex may cause biological toxicity, but we found that the complex was tightly bound within polydopamine and was only minimally released into the surrounding environment.

2. Results and Discussion

Polydopamine was prepared by dissolving dopamine-hydrochloride (2 mg/mL) in a basic buffered solution (10 mM phosphate buffered saline (PBS) pH 8.3). Polydopamine formation was monitored by high-performance liquid chromatography mass spectrometry (HPLC-MS). Two peaks at elution times of 5.0 and 14.4 minutes were detected (**Figure 1**A). The peak at

S. Hong, Y. S. Na, S. Choi, I. T. Song, Prof. W. Y. Kim, Prof. H. Lee
Department of Chemistry
KAIST, 335 Science Rd., Daejeon, 305-701, Korea
E-mail: wooyoun@kaist.ac.kr; haeshin@kaist.ac.kr
Prof. H. Lee
Graduate School of Nanoscience & Technology (WCU) and KAIST Institute for NanoCentury
KAIST, 335 Science Rd., Daejeon, 305-701, Korea

DOI: 10.1002/adfm.201201156

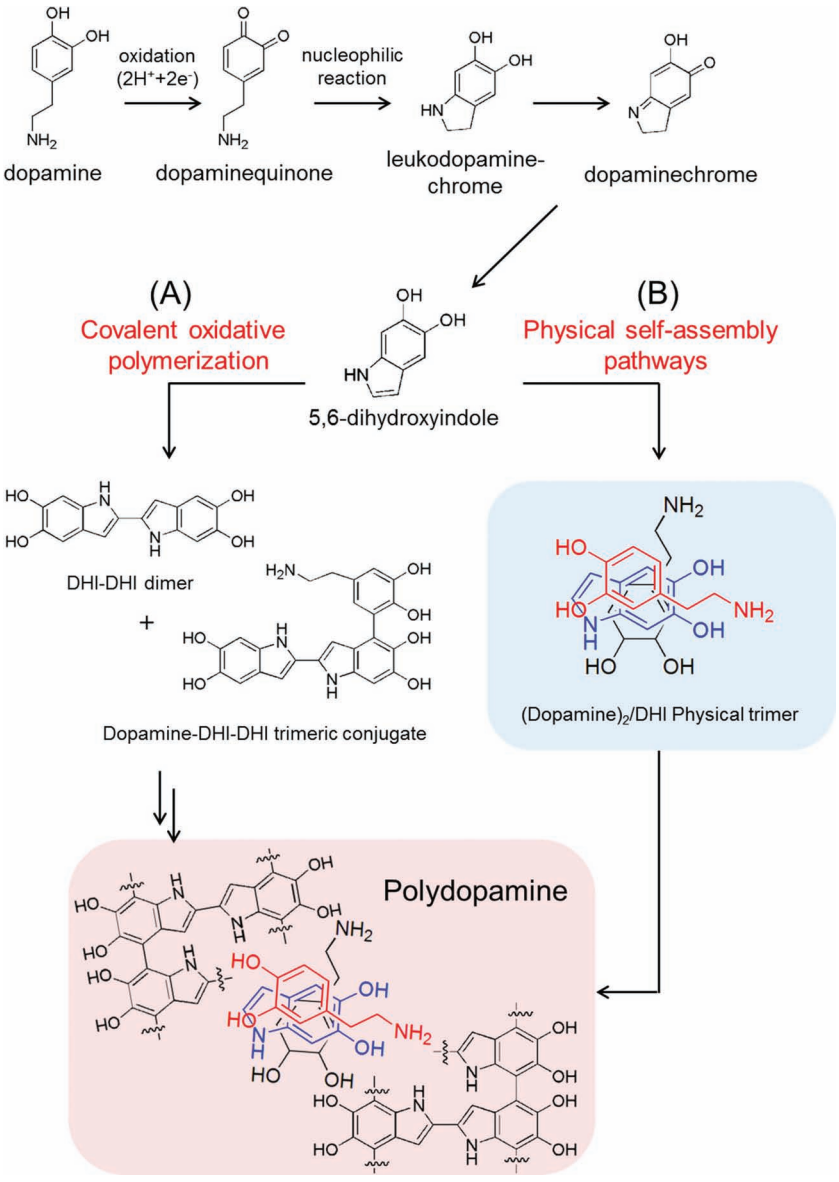

Scheme 1. Polydopamine synthesis occurs via two pathways: A) a pathway of covalent bond-forming oxidative polymerization and B) a newly proposed pathway of physical self-assembly of dopamine and DHI.

5.0 min was unpolymerized dopamine. To increase the amount of the 14.4-min eluent, an oxidizing agent, sodium periodate ($NaIO_4$), was used (0.01 equivalents to dopamine). The elution time was unchanged upon the addition of sodium periodate, indicating that it did not alter the chemical structures of the eluate. Also, the similar chromatographic profiles observed in high-pressure liquid chromatography (HPLC) in the presence or absence of $NaIO_4$ indicated that the polydopamine intermediates were not be significantly altered by the oxidizing agent (Figure S1, Supporting Information). This result is consistent to the previous study in which polydopamine formation is not significantly influenced by the presence of $NaIO_4$.[34] It can be postulated that the result of $(dopamine)_2$/DHI complex formation might be different between PBS (current study) and Tris (original study).[1] We found that the eluate at 14.4 min was consistently detected in Tris buffer (Figure S2, Supporting Information). As a result of the $NaIO_4$ treatment (1 min), the peak area was increased by approximately 40-fold (264.9 mAU → 10136.9 mAU). The HPLC-MS showed that the compound detected at the elution time of 14.4 min had mass-to-charge ratios (m/z) of 454, 325, and 303 (Figure 1B). Subsequently, we collected the eluted solution (14.4 min) from preparation scale liquid chromatography (prep-LC) equipment for further ^{1}H-NMR analysis. ^{1}H-NMR analysis showed all of the protons from both dopamine and DHI (Figure 1C). The three peaks at 6.81, 6.74, and 6.61 ppm (blue) corresponded to the 2-, 5-, and 6-carbons of dopamine. Similarly, the peaks at 7.04, 6.95, 6.87, and 6.20 ppm (red) were the 3-, 7-, 4-, and 2-carbons of DHI. We did not expect the ^{1}H-NMR data to show all of the available ^{1}H peaks from dopamine and DHI because of the high molecular weight detected by MS (e.g., 454 m/z). If the eluted compound had formed the product by oxidative covalent linkages, only a partial spectrum of the ^{1}H-NMR data shown in Figure 1C would have occurred due to the loss of protons from covalent bond formation. The peak area ratio of dopamine (blue) to DHI (red) was 2:1 (Figure 1C). This result indicates that the purified product was a robust, self-assembled trimeric complex of two dopamines and one DHI (Figure 1D). Furthermore, the mass spectrometry results supported the observed self-assembly. The mass peaks at 325 and 303 m/z indicated the physical assembly of dopamine/DHI/Na^+ and dopamine/DHI, respectively (Figure 1E). The peak corresponding to 454 m/z might represent an oxidized form of the $(dopamine)_2$/DHI trimer (mass = 456). The mass difference could result from an oxidation reaction during molecular charging in a gas phase.

We hypothesized that oxidative covalent bonds can be formed by disrupting the self-assembled complex. In this way, it is possible to monitor the reaction of dopamine and DHI to form polydopamine in a controlled manner (i.e., re-initiation of polymerization of dopamine). Solvents, such as dimethyl sulfoxide (DMSO) and acetone, have been known to disrupt hydrogen bonds.[35] Thus, we used a deuterated (d_6-) acetone NMR solvent to dissociate the complex. As expected, we found covalent bond-forming oxidation reactions in the self-assembled $(dopamine)_2$/DHI complex. The reaction was monitored for 41 hours (**Figure 2**A). After 2 h, the doublet peak at 6.2 ppm decreased significantly and completely disappeared after 17 h (right red box). The disappearing peak corresponded to the proton at the 2-carbon of DHI. The doublet at 7.0 ppm (3rd carbon) became a singlet after 17 h (left red box) due to the elimination of proton-proton

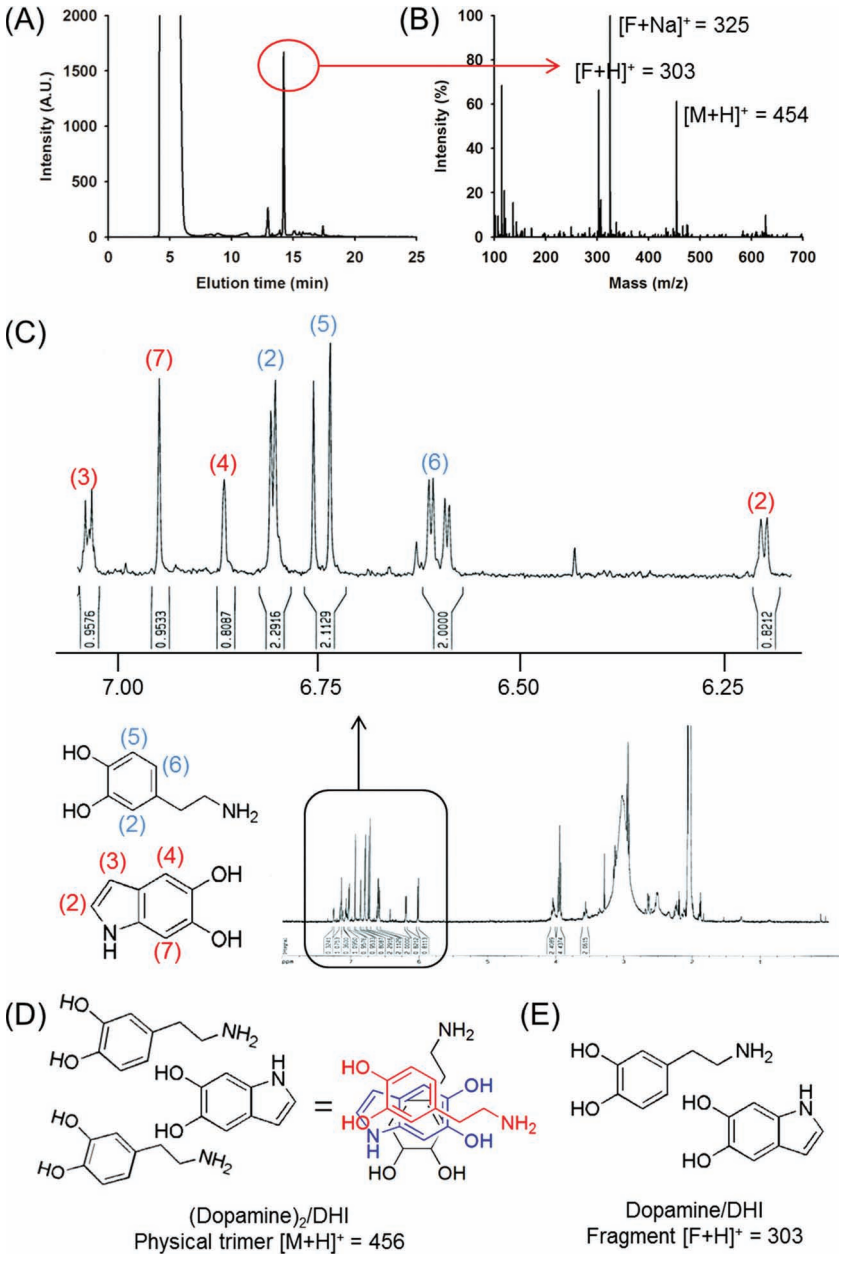

Figure 1. A) HPLC data from a polymerized dopamine solution after a 1 min treatment with $NaIO_4$. B) Mass spectrometry data of the peak eluted at 14.4 min. C) ^{1}H-NMR data of the early intermediate of dopamine polymerization. D) A physical trimer of $(dopamine)_2$/DHI, corresponding to the mass peak of 456 m/z. E) A possible fragment of polydopamine with a mass of 303 m/z.

coupling between the 2- and 3-carbons of DHI. This conversion from a doublet to a singlet confirms that an oxidative reaction occurred at the 2-carbon in DHI, indicating that 2,2-linked DHI-DHI dimer was formed (from Figure 2B,C). Subsequently, the 2,2-linked DHI-DHI dimer further reacted with dopamine to form a trimeric conjugate of dopamine-DHI-DHI (Figure 2D). The 5-carbon of dopamine and 4-carbon of DHI were covalently linked (4,5-dopamine-DHI-DHI), resulting in partial peak separations of the protons linked to the 2- and 6-carbons (blue boxes). The partial separation of peaks indicates that the trimer-forming reaction was not completed after 41 h. The integration values for the peak support the formation of 4,5-dopamine-DHI-DHI. Decreases in the peak area for the 1H connected to the 5-carbon of dopamine, and the one linked to the 4-carbon of DHI were observed (1.8440 → 1.5815 for the 5-carbon of dopamine and 0.7058 → 0.5985 for the 4-carbon of DHI on the basis of an integral value of 2 for the 1H linked to the 2-carbon of dopamine). As the covalent bond-forming oxidation reaction progressed, we found a brown-black precipitation, which was also observed during the polydopamine coating process (Figure 2E). This precipitation might be due to intermolecular assembly such as π–π and other interactions. Therefore, the overall mechanism for the polydopamine formation seems to use two different pathways, self-assembly of dopamine and DHI (i.e., $(dopamine)_2$/DHI) and covalent bond formation, such as dopamine-DHI-DHI conjugates. Further analysis of the oxidation compounds and their formation kinetics needs to be performed.

We built a model interaction to understand the formation of the $(dopamine)_2$/DHI and the precipitation caused by intermolecular interactions. Due to the structure of dopamine and DHI, there are a variety of possible inter-molecular interactions such as ionic, cation-π, π–π, quadrupole-quadrupole and hydrogen bonding (H-bonding) interactions. For investigating non-covalent interactions of the complex, we performed quantum mechanical calculations to quantitatively compare the relative stability between dopamine and DHI. Understanding the dimeric interaction can be extended to the trimeric complex. Four different stable structures were constructed: H- bonding and T-shape interaction (**Figure 3**A), the same H-bond and T-shape interaction with a different molecular configuration (Figure 3B), cation-π and H-bonding (Figure 3C), and cation-π only (Figure 3D). Quantitative description of non-covalent interactions is highly sensitive to the choice of computational methods. Thus, we compared the results from four different methods including Hartree-Fock (HF), density functional theory with hybrid functionals (B3LYP) or dispersion corrected functionals (wb97xd[36] and M06).[37] It has been known that the HF and B3LYP methods lack dispersion interactions. Indeed, both methods underestimated binding energies for the dimer structures in Figure 3 as compared to the others (**Table 1**). The wb97xd produced the largest binding energies among others in both gas and aqua phases, and the values are reasonable as compared to typical cation-pi interactions.[38] The M06 yielded a bit smaller energies within 3 ~ 4 kcal mol^{-1} than the wb97xd.

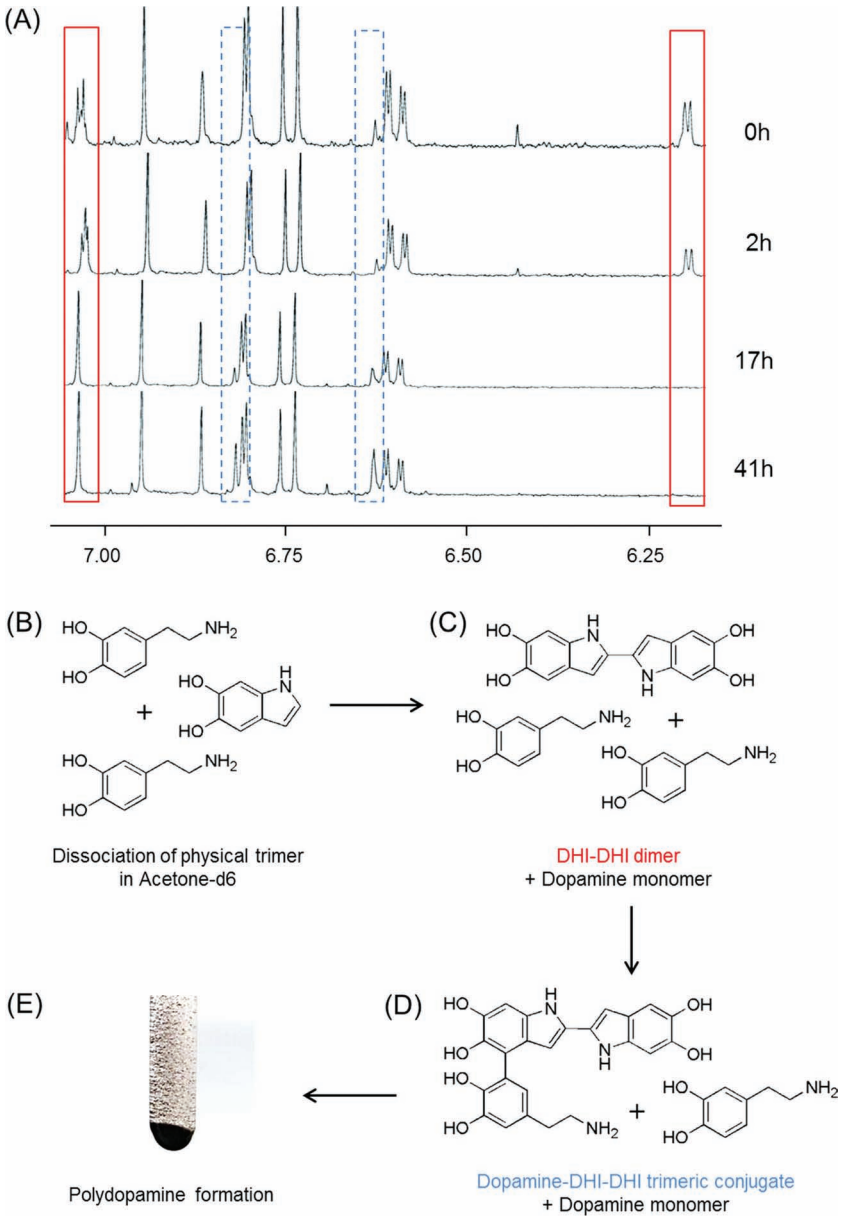

Figure 2. A) ^{1}H-NMR data for monitoring covalent bond-forming reaction of dopamine and DHI for 0 h, 2 h, 17 h, and 41 h in acetone-d_6 NMR solvent. B) The dissociated dopamine and DHI from the self-assembled trimer in acetone-d_6 to re-initiate the covalent bond-forming oxidation reaction. C) The DHI-DHI dimer and D) the dopamine-DHI-DHI trimeric conjugate. E) Polydopamine brown-black precipitation formed by breaking the physical trimer.

Solvation effects were significant for all the cases. In particular, for the wb97xd and M06 results, it lowered the binding energies by about two or three times. However, the binding energies are still very high (~10 kcal mol^{-1}) in aqua phase, which supports the formation of stable complexes between the dopamine and DHI. Hereafter all the discussions are based on the wb97xd results. Interestingly, the model (A) in Figure 3 was the most stable in both gas and aqua phases. It incorporates a T-shape interaction between the hydrogen atom in a hydroxyl group of the dopamine and the aromatic ring in the DHI as well as a hydrogen bonding between the oxygen in a hydroxyl group of the DHI and a hydrogen in the amine group of the dopamine. The model (C), the second lowest one, contains not only a cation-pi interaction between the amine of the dopamine and the aromatic ring of the DHI, but also a hydrogen bonding between hydroxyl groups from each compound. The model (B), the third one, have similar interactions with the model (A), but a hydrogen of the phenyl ring of the dopamine instead of that in a hydroxyl group participates in the T-shape interaction. The former hydrogen is less positive than the latter one, resulting in the slightly smaller binding energy. The model (D) solely with a cation-pi interaction is less stable than the others. The results showed that the combination of the H-bonding and T-shape interactions are favorable, and particularly the structure shown in Figure 3a was shown to be the most stable. Other types of interactions including the cation-π may also contribute to the formation of stable complexes (Table 1). Recently, Dreyer et al. reported that polydopamine consists of non-covalent assembly of dopamine and its oxidized monomers.[39] This result is different from the report herein in the sense that polydopamine is formed not only by non-covalent self-assembly but covalent linkages. The differences in the proposed structures should be further investigated for scientific clarification.

Previous studies have demonstrated that polydopamine shows minimal toxicity in vitro and in vivo.[8,11] Polydopamine-functionalized substrates attenuate the in vivo toxicity of materials by increasing the hydrophilicity of the tissue-contacting interfaces. In vitro, the pDA-functionalized surfaces facilitate cell adhesion and proliferation in a material-independent manner. Therefore, we hypothesized that the dopamine found in the self-assembled complex can affect biocompatibility, but a low-level release of dopamine from the self-assembled $(dopamine)_2$/DHI complex could explain the excellent biocompatibility demonstrated in previous research.[8,11] In fact, dopamine can trigger a variety of biological signals to cause cellular toxicity.[40] To prove this hypothesis, polydopamine-coated silica beads (pDA-beads) were used for quantitative analysis. The total amount of polydopamine coated on 100 mg of silica beads was 1257 μg, as determined by thermogravimetric analysis (TGA). To determine the amount of the entrapped dopamine, 5 M HCl was applied to the pDA-beads to cause disassembly. In this acidic condition, all physically assembled molecules are dissociated. We found that a significant amount (14.2% (w/w)) of unpolymerized dopamine was entrapped in the polydopamine. Subsequently, we measured the amount of dopamine released from the coated beads using HPLC (elution time = 5.0 min), with a standard curve

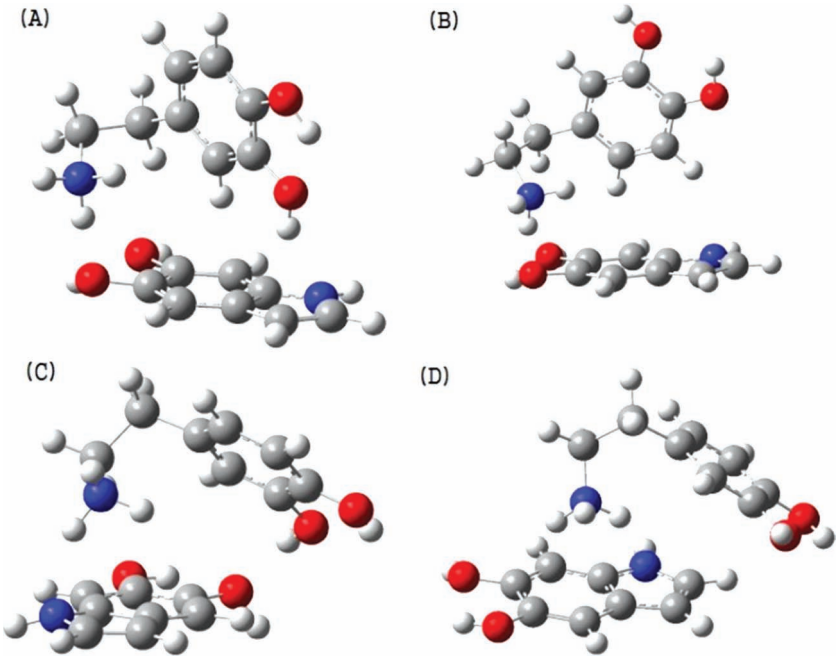

Figure 3. Four representative stable structures of $[F+H]^+$. Each structure contains different types of interactions. For example, A,B) hydrogen bonding and T-shape interactions, C) hydrogen bonding and cation-pi interactions, and D) only cation-pi interaction.

3. Conclusion

In summary, we identified the self-assembled $(dopamine)_2$/DHI physical complexes during polydopamine preparation. This is the first report that there is a physical self-assembly pathway contributing to the known covalent bond-forming oxidative polymerization of dopamine. Our study provides a new perspective on polydopamine structures that can potentially influence our current views on bio-pigments such as melanins.

4. Experimental Section

HPLC Analysis of Pre-Intermediates and Collection of a Major Intermediate by Prep-LC: 20 mg of dopamine hydrochloride (Sigma Aldrich, USA) was dissolved in 1 mL of 1XPBS, pH 8.30 adjusted. 10 µL of sodium periodate ($NaIO_4$, Sigma Aldrich, USA) solution at 20 mg mL^{-1} concentration in distilled water was added to the dopamine solution. After 1 min for mixing, the reaction solution was 0.2 µm syringe filtered (Minisart, Sartorius stedim biotech, USA) and then 100 µL of solution was injected to the HPLC equipment. HPLC analysis was performed with the Agilent 1200 Infinity Series

of dopamine (Figure S3, Supporting Information) and found that only 1.7% (w/w) of dopamine was released (**Figure 4**A, 3rd bar). As we hypothesized, the concentration of dopamine released from the pDA-beads was very low: 19.4 µg mL^{-1} from 100 mg/mL of the beads. In these conditions, the cultured cells were highly viable (>90%, Figure 4B). We prepared various concentrations of dopamine-containing media and found that a dopamine concentration of 300 µg mL^{-1} began to show cytotoxic effects (Figure S4, Supporting Information). Additionally, suspending more than 100 mg/mL of pDA-beads is unrealistic in many practical mammalian cell-involved experiments. The growth and morphology of the cultured cells were completely normal after 24 h of incubation with 100 mg/mL concentration of pDA-beads (Figure 4C). Thus, the experiment supports our hypothesis that the self-assembled $(dopamine)_2$/DHI complex is tightly entrapped in the polydopamine, exhibiting extremely low-level release of the unpolymerized dopamine, which explains the low-level cytotoxicity of the polydopamine.

Table 1. Binding energy in gas phase and aqua solution phase of the dimers in Figure 3 (unit: kcal/mol).

Model	A		B		C		D	
Phase	Solution	Gas	Solution	Gas	Solution	Gas	Solution	Gas
HF	−4.5	−20.6	−4.2	−19.5	−4.0	−17.1	−1.2	−19.1
b2lyp	−6.7	−22.5	−5.5	−20.9	−3.9	−17.3	−2.1	−16.2
wb97xd	−14.4	−30.9	−11.7	−28.1	−13.1	−27.8	−10.6	−23.7
M06	−11.8	−27.9	−9.6	−25.5	−9.9	−24.4	−7.3	−20.3

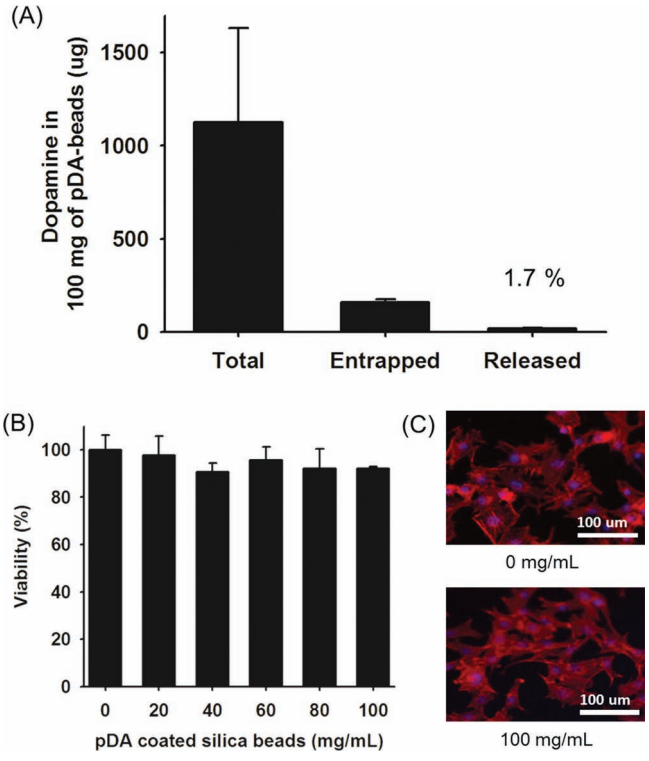

Figure 4. A) Totally coated amounts of polydopamine on 100 mg of silica beads (left), unpolymerized dopamine (middle), and released dopamine in 1× PBS pH 7.4 for 24 h (right). B) Cell viability after 24 h incubation with the released dopamine from pDA-beads. C) Cell morphology after 24 h incubation without (upper) and with 100 mg/mL of the pDA-beads (lower).

LC system containing column unity, degasser, quaternary pump, auto-sampler, and UV detector. Discovery BIO wide pore C18 column, 3 μm (Supelco Analytical, USA) using mixtures of distilled water with 0.1% tetrafluoroacetic acid (TFA) and acetonitrile (ACN) with 0.1% TFA was used. The flow was 0.5 mL/min and separated reaction sample was detected by UV-Vis at 280 nm. For collecting the major intermediate, Agilent 1100 Series Prep-LC system containing column unity, binary pump, auto-sampler, UV detector and auto-collector was used. Dopamine and $NaIO_4$ mixture was prepared the same as for previous HPLC analysis. The injection volume was 500 μL and flow was 10 mL min^{-1}. The column was Discovery BIO wide pore C18 column, 10 μm (Supelco Analytical, USA), the same condition as for HPLC analysis except for the enlarged amount scale. We repeated this collection step more than twenty times for the sufficient amount of product for ^{1}H-NMR analysis (>1 mg).

1H-NMR Analysis of a Purified Self-Assembled Physical Intermediate: The chemical structure of a collected intermediate in dopamine polymerization was investigated by ^{1}H NMR using Bruker AVANCE 400 spectrometer in acetone-d_6 solutions. The data was measured after 0 h, 2 h, 17 h, and 41 h for determining the peak changes.

Preparation of pDA-Coated Silica Beads: 3 g of silica gel 60 (for column chromatography usage from Merck, size: 40–63 μm) was dispersed in 30 mL of a 2 mg mL^{-1} dopamine solution in 1× PBS, and the pH was adjusted to pH 8.3. The reaction solution was mixed by an inverting method for 15 h. The reaction solution was subsequently filtered by using a glass filter with DDW washing. The filtered silica beads was lyophilized and then used for the cytotoxicity test of pDA-released dopamine.

Cytotoxicity Test of pD-Released Dopamine: NIH3T3 fibroblast cells were seeded onto 96-well plate with 1×10^4 cells $well^{-1}$ density and cultured in DMEM media with 10% FBS at 37 °C, 5% CO_2. After 24 h, free and pDA-released dopamine was added to media and incubated another 24 h with same culture condition. Free dopamine with concentration of 1, 0.3, 0.1, 0.03 and 0 mg was added to 1 mL of cell culture media for testing cytotoxicity of free dopamine. For testing cytotoxicity of pDA-released dopamine, 20, 40, 60, 80 and 100 mg of pDA-coated silica beads was added to 1 mL of cell culture media and incubated for 24 h. Each case, MTT assay was performed after 24 h for cell viability test after dopamine contact. 200 μL of media with 20 μL of MTT agent was added to each well and incubated for 2 h. After removing the media, 200 μL of DMSO was added for dissolving the water-insoluble assay product. UV absorbance of assay product was measured at 570 nm with micro-plate reader, Bio-Rad Model 550. For cell imaging, nuclei was stained by VECTASHIELD mounting solution with DAPI (Vector Laboratories, USA) after actin staining by Rhodamin phaloidin (Invitrogen, USA).

Computational Method: Gaussian 09 package with different levels of theory (described below) and the 6–31+G* basis set have been used for all the computations.[41] The solvation effect in aqua phase was taken into account by the conductor-like polarizable continuum model.[42] While the complexes are composed of dimers, trimers, and probably higher orders, here we only concern about the dimers as a prototype to figure out plausible interaction types. We first optimized dimer structures in gas phase, and further stabilized them in aqua condition. Figure S5 (Supporting Information) shows four representative structures we found. The binding energies (BE) of the dimers were evaluated as follows: BE = E(Dimer)-{E(DHI)+E(DopamineH^+)}

Supporting Information

Supporting Information is available from the Wiley Online Library or from the author.

Acknowledgements

This work was financially supported by National Research Foundation of South Korea: WCU Program (R31-10071), Basic Science Research Program (2012-0000909), Bio & Medical Technology Development Program (2012-0006085), and Fostering Core Leaders of the Future Basic Science Program (2012H1A8002613). H.L. and W.Y.K are also grateful for financial support from Chung-Am Fellowship.

Received: April 26, 2012
Revised: June 12, 2012
Published online: July 5, 2012

[1] H. Lee, S. M. Dellatore, W. M. Miller, P. B. Messersmith, *Science* **2007**, *318*, 426.
[2] J. Ryu, S. H. Ku, H. Lee, C. B. Park, *Adv. Funct. Mater.* **2010**, *20*, 2132.
[3] M. Lee, S. H. Ku, J. Ryu, C. B. Park, *J. Mater. Chem.* **2010**, *20*, 8848.
[4] W. Yang, P. Thordarson, J. J. Gooding, S. P. Ringer, F. Braet, *Nanotechnology* **2007**, *18*, 412001.
[5] S. H. Yang, S. M. Kang, K. B. Lee, T. D. Chung, H. Lee, I. S. Choi, *J. Am. Chem. Soc.* **2011**, *133*, 2795.
[6] S. M. Kang, I. You, W. K. Cho, H. K. Shon, T. G. Lee, I. S. Choi, J. M. Karp, H. Lee, *Angew. Chem. Int. Ed.* **2010**, *49*, 9401.
[7] H. Lee, B. P. Lee, P. B. Messersmith, *Nature* **2007**, *448*, 338.
[8] S. H. Ku, J. Ryu, S. Hong, H. Lee, C. B. Park, *Biomaterials* **2010**, *31*, 253.
[9] S. H. Ku, J. S. Lee, C. B. Park, *Langmuir* **2010**, *26*, 15104.
[10] T. S. Sileika, H. D. Kim, P. Maniak, P. B. Messersmith, *ACS Appl. Mater. Interfaces* **2011**, *3*, 4602.
[11] S. Hong, K. Y. Kim, H. J. Wook, S. Y. Park, K. D. Lee, D. Y. Lee, H. Lee, *Nanomedicine* **2011**, *6*, 793.
[12] J. Cui, Y. Wang, A. Postma, J. Hao, L. Hosta-Rigau, F. Caruso, *Adv. Funct. Mater.* **2010**, *20*, 1625.
[13] Q. Liu, B. Yu, W. Ye, F. Zhou, *Macromol. Biosci.* **2011**, *11*, 1227.
[14] D. Losic, Y. Yu, M. S. Aw, S. Simovic, B. Thierry, Addai-Mensah, *Chem. Commun.* **2010**, *46*, 6323.
[15] Y. Ren, J. G. Rivera, L. He, H. Kulkarni, D. K. Lee, P. B. Messersmith, *BMC Biotechnol.* **2011**, *11*, 63.
[16] G. Wang, H. Huang, G. Zhang, X. Zhang, B. Fang, L. Wang, *Langmuir* **2011**, *27*, 1224.
[17] H. Hu, B. Yu, Q. Ye, Y. Gu, F. Zhou, *Carbon* **2010**, *48*, 2347.
[18] M. H. Ryou, Y. M. Lee, J. K. Park, J. W. Choi, *Adv. Mater.* **2011**, *23*, 3066.
[19] K. Kang, I. S. Choi, Y. Nam, *Biomaterials* **2011**, *32*, 6374.
[20] W. Ye, D. Wang, H. Zhang, F. Zhou, W. Liu, *Electrochim. Acta* **2010**, *55*, 2004.
[21] R. Liu, S. M. Mahurin, C. Li, R. R. Unocic, J. C. Idrobo, H. Gao, S. J. Pennycook, S. Dai, *Angew. Chem. Int. Ed.* **2011**, *50*, 6799.
[22] W. Ye, H. Hu, H. Zhang, F. Zhou, W. Liu, *Appl. Surf. Sci.* **2010**, *256*, 6723.
[23] Y. Weng, Q. Song, Y. Zhou, L. Zhang, J. Wang, J. Chen, Y. Leng, S. Li, N. Huang, *Biomaterials* **2011**, *32*, 1253.
[24] H. Lee, J. Rho, P. B. Messersmith, *Adv. Mater.* **2009**, *21*, 431.
[25] C. Y. Li, W. C. Wang, F. J. Xu, L. Q. Zhang, W. T. Yang, *J. Membrane Sci.* **2011**, *367*, 7.
[26] Q. Ye, F. Zhou, W. Liu, *Chem. Soc. Rev.* **2011**, *40*, 4244
[27] J. H. Waite, *Nat. Mater.* **2008**, *7*, 8.
[28] T. J. Park, J. Kim, T. K. Kim, H. M. Park, S. S. Choi, Y. Kim, *Bull. Korean Chem. Soc.* **2008**, *29*, 2459.
[29] B. B. Adhyaru, N. G. Akhmedov, A. R. Katritzky, C. R. Bowers, *Magn. Reson. Chem.* **2003**, *41*, 466.
[30] M. Arzillo, A. Pezzella, O. Crescenzi, A. Napolitano, E. Land, V. Barone, M. d'Ischia, *Org. Lett.* **2010**, *12*, 3250.
[31] M. Bisaglia, S. Mammi, L. J. Bubacco, *Biol. Chem.* **2007**, *282*, 15597.
[32] M. d'Ischia, A. Napolitano, A. Pezzella, P. Meredith, T. Sarna, *Angew. Chem. Int. Ed.* **2009**, *48*, 3914.

[33] V. Ball, D. D. Frari, M. Michel, M. J. Buehler, V. Toniazzo, M. K. Singh, J. Gracio, D. Ruch, *BioNanoSci*. **2012**, *2*, 16.
[34] Q. Wei, F. Zhang, J. Li, B. Li, C. Zhao, *Polym. Chem.* **2010**, *1*, 1430.
[35] M. Perrin, N. Ehlinger, L. Viola-Motta, S. Lecocq, I. Dumazet, S. Bouoit-Montesino, R. J. Lamartine, *Incl. Phenom. Macro.* **2001**, *39*, 273.
[36] J.-D. Chai, M. Head-Gordon, *Phys. Chem. Chem. Phys.* **2008**, *10*, 6615.
[37] Y. Zhao, D. Truhlar, *Theo. Chem. Acc.* **2008**, *120*, 215.
[38] J. C. Ma, D. A. Dougherty, *Chem. Rev.* **1997**, *97*, 1303.
[39] D. R. Dreyer, D. J. Miller, B. D. Freeman, D. R. Paul, C. W. Bielawski, *Langmuir* **2012**, *28*, 6428.
[40] M. V. Clement, L. H. Long, J. Ramalingam, B. J. Halliwell, *Neurochemistry* **2002**, *81*, 414.
[41] M. J. Frisch, G. W. Trucks, H. B. Schlegel, G. E. Scuseria, M. A. Robb, J. R. Cheeseman, J. A. Montgomery Jr., T. Vreven, K. N. Kudin, J. C. Burant, J. M. Millam, S. S. Iyengar, J. Tomasi, V. Barone, B. Mennucci, M. Cossi, G. Scalmani, N. Rega, G. A. Petersson, H. Nakatsuji, M. Hada, M. Ehara, K. Toyota, R. Fukuda, J. Hasegawa, M. Ishida, T. Nakajima, Y. Honda, O. Kitao, H. Nakai, M. Klene, X. Li, J. E. Knox, H. P. Hratchian, J. B. Cross, V. Bakken, C. Adamo, J. Jaramillo, R. Gomperts, R. E. Stratmann, O. Yazyev, A. J. Austin, R. Cammi, C. Pomelli, J. W. Ochterski, P. Y. Ayala, K. Morokuma, G. A. Voth, P. Salvador, J. J. Dannenberg, V. G. Zakrzewski, S. Dapprich, A. D. Daniels, M. C. Strain, O. Farkas, D. K. Malick, A. D. Rabuck, K. Raghavachari, J. B. Foresman, J. V. Ortiz, Q. Cui, A. G. Baboul, S. Clifford, J. Cioslowski, B. B. Stefanov, G. Liu, A. Liashenko, P. Piskorz, I. Komaromi, R. L. Martin, D. J. Fox, T. Keith, M. A. Al-Laham, C. Y. Peng, A. Nanayakkara, M. Challacombe, P. M. W. Gill, B. Johnson, W. Chen, M. W. Wong, C. Gonzalez, J. A. Pople, *Gaussian 09 A.1*, Gaussian, Inc., Wallingford, CT **2009.**
[42] M. Cossi, N. Rega, G. Scalmani, V. Barone, *J. Comput. Chem.* **2003**, *24*, 669.